1-1-2009

Water in Comets 71p/Clark and C/2004 B1 (Linear) With Spitzer

Dominique Bockelée-Morvan

Charles E. Woodward

Michael S. Kelley
University of Central Florida

Diane H. Wooden

The Astrophysical Journal, 696:1075–1083, 2009 May 10 doi:10.1088/0004-637X/696/2/1075

WATER IN COMETS 71P/CLARK AND C/2004 B1 (LINEAR) WITH *SPITZER*

Dominique Bockelée-Morvan[1], Charles E. Woodward[2], Michael S. Kelley[3], and Diane H. Wooden[4]
[1] LESIA, Observatoire de Paris, 5 place Jules Janssen, F92195, Meudon, France; dominique.bockelee@obspm.fr
[2] Department of Astronomy, School of Physics and Astronomy, 116 Church Street, S. E., University of Minnesota, Minneapolis, MN 55455, USA; chelsea@astro.umn.edu
[3] Department of Physics, University of Central Florida, 4000 Central Florida Blvd., Orlando, FL 32816-2385, USA; msk@astro.umd.edu
[4] NASA Ames Research Center, MS 245-3, Moffet Field, CA 94035-1000, USA; d.h.wooden@nasa.gov
Received 2008 October 22; accepted 2009 February 3; published 2009 April 22

ABSTRACT

We present 5.5–7.6 μm spectra of comets 71P/Clark (2006 May 27.56 UT, $r_h = 1.57$ AU pre-perihelion) and C/2004 B1 (LINEAR) (2005 October 15.22 UT, $r_h = 2.21$ AU pre-perihelion and 2006 May 16.22 UT, $r_h = 2.06$ AU post-perihelion) obtained with the *Spitzer Space Telescope*. The ν_2 vibrational band of water is detected with a signal-to-noise ratio of 11–50. Fitting the spectra using a fluorescence model of water emission yields a water rotational temperature of < 18 K for 71P/Clark and $\simeq 14 \pm 2$ K (pre-perihelion) and 23 ± 4 K (post-perihelion) for C/2004 B1 (LINEAR). The water ortho-to-para ratio in C/2004 B1 (LINEAR) is measured to be 2.31 ± 0.18, which corresponds to a spin temperature of 26^{+3}_{-2} K. Water production rates are derived. The agreement between the water model and the measurements is good, as previously found for *Spitzer* spectra of C/2003 K4 (LINEAR). The *Spitzer* spectra of these three comets do not show any evidence for emission from polycyclic aromatic hydrocarbons and carbonate minerals, in contrast to results reported for comets 9P/Tempel 1 and C/1995 O1 (Hale-Bopp).

Key words: comets: individual (71P/Clark, C/2004 B1 LINEAR) – infrared: solar system

1. INTRODUCTION

Production rates of volatiles are used to quantify cometary activity and to measure volatile abundances. Water is the dominant ice in cometary nuclei and its sublimation governs the activity of comets at heliocentric distances, r_h, $\lesssim 3$ AU from the Sun. Water production rates, $Q(H_2O)$, the rotational temperature, T_{rot}(K), and the nuclear spin temperature inferred from the water ortho-to-para ratio (OPR) are physical parameters useful in a variety of studies related to cometary atmospheres and cometary physics.

Unlike other constituents of cometary atmospheres, water vapor is difficult to observe directly from the ground because of terrestrial atmospheric absorption. Non-resonance fluorescence vibrational bands (hot bands), not absorbed by telluric H_2O, can be observed from the ground in relatively active comets ($Q(H_2O) \gtrsim$ a few 10^{28} molecules s^{-1}; Disanti & Mumma 2008). The detection of the H_2O fundamental bands of vibration (ν_1, ν_3 at 2.7 μm, ν_2 at 6.3 μm), and of H_2O rotational lines in the submillimeter and far-infrared domains, requires space-based instrumentation. Detection of these signatures has been achieved in the coma of several comets using spectrographs on the VEGA, Deep Impact, and Rosetta spacecrafts, and instruments on the Kuiper Airborne Observatory, the *Infrared Space Observatory* (*ISO*), the *Submillimeter Wave Astronomy Satellite,* and the *Odin* satellite (A'Hearn et al. 2005; Biver et al. 2007; Bockelée-Morvan et al. 2004 and references therein; Gulkis et al. 2007).

The Infrared Spectrograph (IRS; Houck et al. 2004) of the *Spitzer Space Telescope* (Gehrz et al. 2007; Werner et al. 2004) covers the 5.3–40 μm spectral region and enables observations of the ν_2 vibrational band of water vapor at 6.3 μm with a spectral resolution of $\sim$100. This band was detected with *Spitzer* in comet C/2003 K4 (LINEAR) with a high signal-to-noise ratio ($\gtrsim 50$), which enabled a detailed study of the band shape using a fluorescence excitation model, assessment of the radial gradient of emission with cometocentric radius, and the measurement of the rotational temperature and ortho-to-para ratio (OPR) of the detected water (Woodward et al. 2007).

An important by-product of the analysis of the *Spitzer* spectra of comet C/2003 K4 (LINEAR) performed by Woodward et al. (2007) was a search for emissions in excess to the water band in the 5.8–7.6 μm domain, which is rich in spectral signatures of gaseous compounds and minerals. Indeed, Lisse et al. (2006, 2007) reported emission from carbonate minerals at 6.5–7.2 μm and organic (polycyclic aromatic hydrocarbon; hereafter PAH) emission at 6.2 μm in the *Spitzer* spectrum of comet 9P/Tempel after the collision with the *Deep Impact* impactor, and in comet C/1995 O1 (Hale-Bopp) based on their reanalysis of the Crovisier et al. (1997) *ISO* spectrum. The methodology of Lisse et al. (2006, 2007) does not rely on a search of individual signatures but from the decrease of the residual χ^2 after a fit of the whole (5.2–40 μm for *Spitzer* spectra) observed spectrum by a modeled spectrum which can incorporate many constituents. A reanalysis of the *ISO* data of comet Hale-Bopp by Crovisier & Bockelée-Morvan (2008) did not confirm the detection of PAHs reported by Lisse et al. (2006) and suggests that carbonate signatures are at most marginal. After detailed modeling of the water ν_2 emission, the spectra of C/2003 K4 (LINEAR) do not show any evidence for emission from PAHs and carbonate minerals (Woodward et al. 2007). Carbonates have been identified in very tiny quantities in the dust grains collected in the coma of 81P/Wild 2 by the *Stardust* spacecraft (Wirick et al. 2007). PAHs have been also detected in *Stardust* samples (Sandford et al. 2006), but a substantial portion of this material may not be of cometary origin (Sandford & Brownlee 2007; Spencer & Zare 2007). PAHs were tentatively identified in near-IR and near-UV cometary spectra, but these detections are controversial (see the discussion in Bockelée-Morvan et al. 2004).

Here, we present long-slit *Spitzer* spectroscopic observations of comets 71P/Clark and C/2004 B1 (LINEAR). Observations in the 5.3–7.6 μm spectral region are presented in Section 2. The data are analyzed with an H_2O fluorescence model using

the same methodology described in Woodward et al. (2007), and the results are presented in Section 3. Residual emissions are discussed in Section 3.6. We conclude the paper in Section 4.

2. OBSERVATIONS AND REDUCTION

Comet 71P/Clark was discovered on 1973 June 09 by Michael Clark at Mount John University Observatory in New Zealand. This comet, with an orbital period of 5.52 years, belongs to the dynamical class of Jupiter-family comets. Its last perihelion approach was on 2006 June 06.80 (perihelion distance $q = 1.562$ AU). Little information is available on this comet in the literature. The radius of its nucleus has been estimated to 0.68 ± 0.07 km from observations with the *Hubble Space Telescope* obtained at $r_h = 2.62$ AU to 1.3 km from observations at $r_h = 4.67$ AU performed with the Keck telescope, suggesting an elongated nucleus with an axis ratio $a/b \gtrsim 2.85$ (Lamy et al. 2004; Meech et al. 2004). The orbit of this comet is peculiar. 71P has a nonzero, nongravitational thrust in the direction normal to the orbital plane (the A_3 nongravitational parameter) that is well determined with good confidence (e.g., Sekanina 1993; Nakano 2006a, 2006b). Erratic time variability of the nongravitational parameters over nucleus revolutions were interpreted as due to a change in the surface distribution of active areas and of the orientation of the spin axis (Sekanina 1993; Szutowicz 1999). The water production rate of 71P/Clark at perihelion in 1973 and 1984 was estimated to be 8–9×10^{27} molecules s^{-1} based on its visual brightness (Sekanina 1993). Woodward et al. (2008) find strong evidence for CO and CO_2 gaseous emission near 4.5 μm in the extended coma pre-perihelion ($r_h = 1.607$ AU) during the 2006 apparition. The *Spitzer* IRS observations of 71P/Clark were conducted $\approx$ 10 days before its 2006 perihelion passage.

Comet C/2004 B1 (LINEAR), first identified as an asteroidal object with a visual magnitude of 19.1 on 2004 January 29.16 UT at a $r_h \simeq 8.1$ AU, was discovered by Young (2004) to be a comet on 2004 January 30.1 UT with a 3″ coma, and an extended tail ($\approx 4''$, PA $\simeq 310°$). Orbital elements derived from astrometric observations (Marsden 2004) and subsequently refined over a data arc spanning years 2004 through 2007 (1779 observations), indicate that this comet is dynamically new, highly inclined to the ecliptic ($i \simeq 114°$), with a perihelion of 2006 February 07.89 UT with a periapsis, $q = 1.602$ AU. Although a relatively bright comet, few ground-based observations are currently reported in the literature. Bonev et al. (2007) conducted *R*-band imaging observations of C/2004 B1 (LINEAR) over a $\sim$ 60 day period between 2006 June and 2006 August, reporting that the comet underwent episodes of variable activity on timescales of days, with a dust production rate (A'Hearn et al. 1984), $Af\rho \simeq 200$–350 cm. The comet also exhibited a substantial coma ($\approx 2 \times 10^4$ km diameter) near the end of 2006 June, and slowly faded in *R* brightness, from $\simeq 14.3$ mag to $\simeq 15.1$ mag, 193 days after perihelion.

2.1. Spitzer IRS

Comet 71P/Clark was observed once ($r_h = 1.565$ AU, a *Spitzer*-comet distance of 0.920 AU, and a phase angle of 37.°8) in the second order of the short-wavelength, low-resolution module (SL2) on 2006 May 27.56 UT as part of a large *Spitzer* Cycle 2 comet survey, program identification (PID) 20021 (PI: C.E. Woodward), astronomical observation request (AOR) key 13818368, and processed with IRS reduction pipeline S15.3.0. The SL2 slit is 3.″7 wide and provides 57″ of spatially resolved spectra (1.″85 pixel^{-1}) with a spectral dispersion of 0.06 μm. Nine spectra (60 s × 5 cycles) at 5.2–7.6 μm were recorded in a 3 × 3 spectral map (executed with no peak-up), with 2.″47 × 38.″0 steps (perpendicular × parallel to the long-slit dimension). The comet was also observed with the long-wavelength, low-resolution (LL) module of IRS, which we used to verify the pointing of the spacecraft. Further analysis of the LL spectrum is beyond the scope of this paper.

Comet C/2004 B1 (LINEAR) was observed twice, both pre- and post-perihelion with the SL2 module as part of a multicycle *Spitzer* initiative to investigate the heliocentric evolution and activity of a given comet, PID 20104 (PI: D.H. Wooden). The SL2 spectra discussed here were derived from IRS spectral mapping observations obtained on 2005 October 15.22 UT (pre-perihelion, $r_h = 2.210$ AU) AOR key 15787008, and on 2006 May 16.24 UT (post-perihelion, $r_h = 2.058$ AU), AOR key 15791616. Pre-perihelion, three spectra (240 s × 5 cycles) were obtained from a 3 × 1 spectral map, while post-perihelion five spectra (60 s × 3 cycles) were generated from a 5 × 1 spectral map. Both AORs were executed using a mapping footprint of 2.″50 steps (perpendicular to the long-slit dimension) with no peak-up on the comet nucleus, accompanied by appropriate shadow (background) observations. Spectral observations of comet C/2004 B1 (LINEAR) using the short-high (SH, 9.9–19.6 μm) module were also obtained, although detailed analysis of these spectra are beyond the scope of this manuscript.

A reconstruction of the pointing for the 71P/Clark SL2 spectral maps indicates that there is an 8″ perpendicular offset between the SL2 extraction position and the JPL Horizons[5] ephemeris position of the comet nucleus at the epoch of our observations, Figure 1(c). This offset is confirmed by comparing the peak in the observed surface brightness distribution in the long-low (LL2, 14–20 μm) cube which is nearly coincident with the Horizons position, Figure 1(d). The spectral maps for both IRS pointings of C/2004 B1 (LINEAR) encompassed the peak in the surface brightness of the coma (Figure 1), hence SL2 extraction apertures centered on the nucleus are possible.

The reduction of the spectra and wavelength calibration of the SL2 data follows the formalism discussed in detail by Kelley et al. (2006) and Woodward et al. (2007). "Hot-pixels" occasionally present in individual extractions derived from the spectral maps were removed and replaced by nearest neighbor interpolation, or ignored altogether. A summary of comet physical parameters, spectral extraction apertures, and derived water production rates (see Section 3) is given in Table 1.

3. DATA ANALYSIS

3.1. Model Fitting of the ν_2 Water Band

As for C/2003 K4 (LINEAR), features observed between 5.8 and 7 μm above the continuum background in the 71P/Clark and C/2004 B1 (LINEAR) *Spitzer* spectra (Figure 2) coincide with the rovibrational structure of the ν_2 water band at the resolution of the short-low (SL2) spectrometer. In order to study whether water band emission fully accounts for the signal in excess of the continuum, these spectra were analyzed using a model of fluorescence water emission following the procedure described in Woodward et al. (2007). Details on the method, model and assumptions can be find in Woodward et al. (2007).

In summary, we use the model of fluorescence water emission presented by Bockelée-Morvan & Crovisier (1989) which

[5] http://ssd.jpl.nasa.gov/horizons.cgi

Table 1
Water in Comets: Model Fits and Production Rates

Obs Date (UT)	α[a] (deg)	r_h (AU)	$\Delta_{Spitzer}$[b] (AU)	Extraction ($'' \times ''$)	Band Intensity[c] (10^{-21} W cm^{-2})	T_{rot} (K)	OPR	(χ^2_ν)[d]	Q_{H_2O} (10^{27} molecules s^{-1})
71P/Clark									
2006 May 27.56	37.8	1.57	0.92	3.7 × 17.9[e]	17.0 ± 1.29	5 ± 13	3.0[f]	0.90	10.43 ± 0.79
C/2004 B1 (LINEAR)									
2005 Oct 15.22	27.5	2.21	2.03	3.7 × 17.9	13.74 ± 0.28	13.6 ± 2.1	2.31 ± 0.18	0.97	10.32 ± 0.21
2006 May 16.22	28.7	2.06	1.61	3.7 × 17.9	9.20 ± 0.82	23 ± 4	2.3[f]	0.90	4.74 ± 0.42

Notes.
[a] Phase angle (defined as vertex angle of Sun–Comet–*Spitzer*).
[b] Distance to *Spitzer* spacecraft.
[c] Band intensity between 5.8 μm and 7 μm.
[d] Reduced χ^2 between 5.85 μm and 7 μm.
[e] Offset with respect to the nucleus position by $\sim 8''$ (see Section 2).
[f] Assumed.

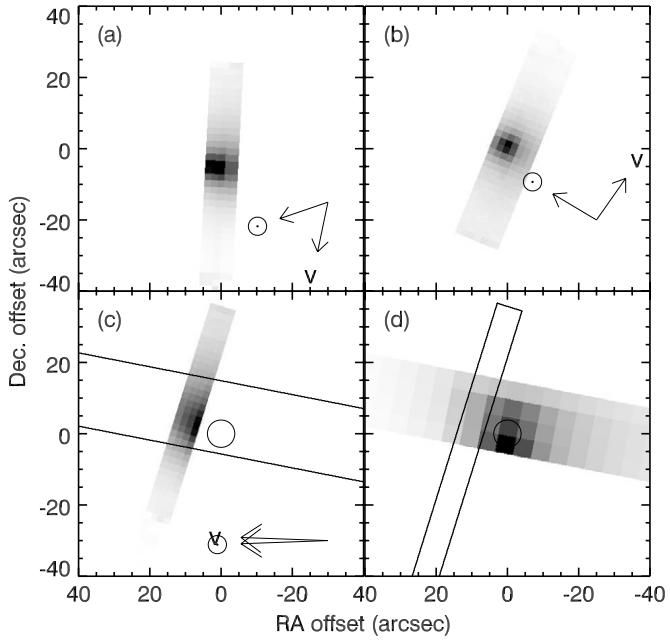

Figure 1. Gray-scale surface-brightness images derived from *Spitzer* IRS spectral mapping data cubes of comets C/2004 B1 (LINEAR) and 71P/Clark: (*a*) IRS short-low order 2 (SL2; 5.3–7.5 μm) observation of comet C/2004 B1 (LINEAR) at $r_h = 2.2$ AU (pre-perihelion); (*b*) IRS SL2 observation of comet C/2004 B1 (LINEAR) at $r_h = 2.1$ AU (post-perihelion); (*c*) IRS SL2 observation of comet 71P/Clark at $r_h = 1.6$ AU (pre-perihelion); (*d*) IRS long-low order 2 (LL2; 14–20 μm) observation of comet 71P/Clark obtained as part of the same *Spitzer* AOR used to acquire the SL2 observation of panel (*c*). Arrows in panels (*a*), (*b*), and (*c*) delineate the projected sun (⊙) and comet velocity (v) directions. The 71P/Clark SL2 observation did not cover the comet nucleus; however, the LL2 observation did. To emphasize this point, we have marked the JPL/Horizons ephemeris position of comet 71P/Clark with a circle, and placed outlines of the LL2 and SL2 modules in panels (*c*) and (*d*), respectively. Spectral extractions discussed in Section 2 are centered on the peak of the surface brightness distribution.

considers five excited vibrational states and their subsequent radiative cascades. Indeed, the ν_2 band, which dominates the water spectrum in the 5.8–7.1 μm spectral region, is significantly populated by radiative decay from higher excited vibrational states. The resulting emission rate of ν_2 is 2.41×10^{-4} s^{-1} at $r_h = 1$ AU from the Sun. For computing the line-by-line fluorescence, 32 ortho and 32 para rotational levels are considered in each vibrational state. The rotational populations in the ground vibrational state is described by a Boltzmann distribution at a temperature T_{rot}. The gas expansion velocity, v_{exp}, was fixed to 0.8 km s^{-1} and the water photodissociation rate was taken equal to 1.6×10^{-5} s^{-1} ($r_h = 1$ AU). These parameters influence to a small extent the retrieved water production rates.

From the model output, synthetic *Spitzer* spectra are generated by convolving the intensity of the individual rovibrational lines with the instrumental spectral response of the spectrometer. The spectral resolution is determined to be 0.0614 ± 0.0027 μm from the pre-perihelion spectrum of C/2004 B1 (LINEAR), in good agreement with the SL2 spectral resolution (0.0605 μm) cited in the *Spitzer* IRS Data Hand Book v.3.2.[6] Our derived value is used for the analysis of the comet spectra in this paper. A slightly higher value of the SL2 spectral resolution, 0.065 μm (determined from the wavelength calibration at the SL2 slit edge), was used in the analysis of the C/2003 K4 (LINEAR) spectra as spectral extractions of this comet were performed near the edge of the slit (see Sections 2.2 and 3.1 in Woodward et al. 2007).

The observed spectra are fitted with a composite curve consisting of the modeled water spectrum superimposed on a fifth-degree polynomial. This latter polynomial determines the underlying continuum due to dust emission. The best-fit modeled spectrum is searched for by applying a least-squares method that uses the gradient-search algorithm of Marquardt. The only free parameters of the model are the water production rate $Q(H_2O)$ (or equivalently, the water column density), T_{rot}, the ortho-to-para ratio (OPR), and the polynomial for the continuum. However, the signal-to-noise ratio in the spectra of comets 71P/Clark and C/2004 B1 (LINEAR) post-perihelion is not high enough to constrain the OPR, so this parameter was fixed when analyzing these data.

Figure 2 shows the model fits superimposed on the observed spectra. In the right panels, B, D, and F, the continuum has been subtracted. The intensity of the water band in continuum-subtracted spectra and the retrieved T_{rot}, OPR and $Q(H_2O)$ are given in Table 1.

As discussed in Woodward et al. (2007), the spectral resolution of *Spitzer* SL2 is too low to resolve the individual ortho and para water lines. Thus a fully independent estimate of the OPR and T_{rot} cannot be derived. However, a robust determination of these parameters is possible from model fitting and χ^2 minimization, because several para lines (near 6.12 and 6.4 μm) are well separated in wavelength from strong ortho lines, while several peaks, dominated by ortho lines, have their relative intensities essentially influenced by T_{rot}. Spectra obtained with high

[6] http://ssc.spitzer.caltech.edu/IRS/dh

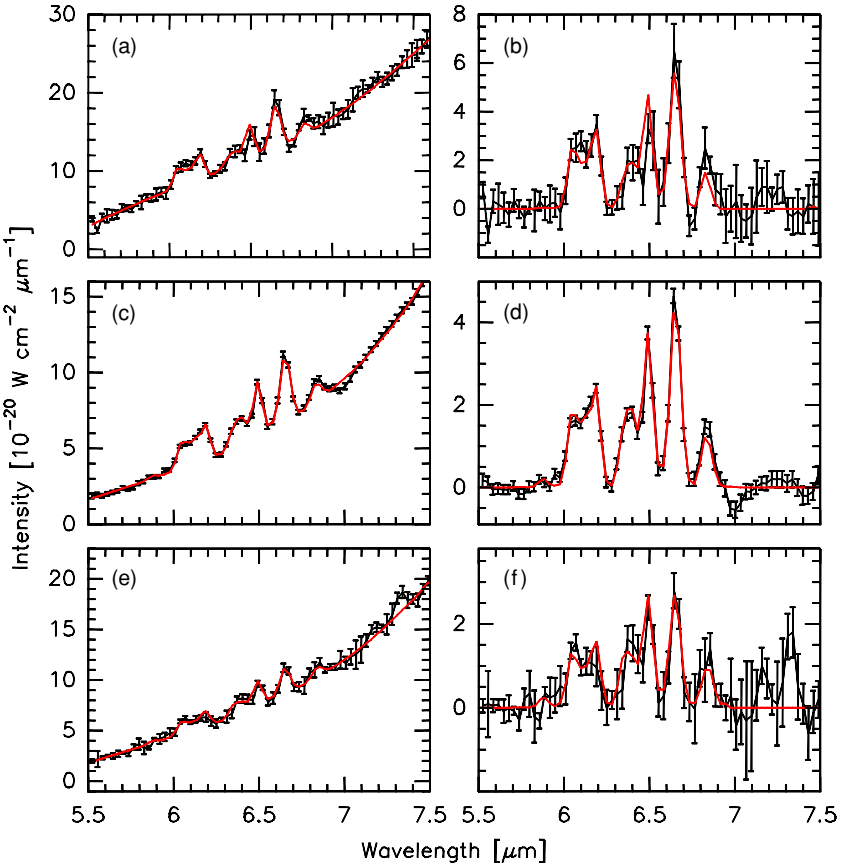

Figure 2. Model fits to the spectra of 71P/Clark (*a*, *b*) and C/2004 B1 (LINEAR) pre-perihelion (*c*, *d*) and post-perihelion (*e*, *f*) observed with *Spitzer* on 2006 May 27.56 UT, 2005 October 27.56 UT and 2006 May 16.22 UT, respectively. The extraction aperture is 3.″7 × 17.″9. Data are shown in black, with the model fits of water emission (in red) superimposed. For 71P/Clark and C/2004 B1 (LINEAR) post-perihelion, model fitting was performed with the rotational temperature $T_{\rm rot}$ taken as a free parameter, and the OPR = 3. In contrast, for the pre-perihelion spectrum of C/2004 B1 (LINEAR), the fit was obtained with both the OPR and $T_{\rm rot}$ taken as a free parameters. The underlying continuum, described by a polynomial of degree 5, was also fitted simultaneously. In panels B and D, the fitted continuum background has been subtracted.

signal-to-noise ratios are of course requisite. Figure 3(a) shows iso-χ^2 contours in the ($T_{\rm rot}$, OPR) region that provides the best fit to the C/2004 B1 (LINEAR) pre-perihelion spectrum. The coefficients of the polynomial describing the continuum background have been set to the values of the best fit. The reduced χ^2 obtained for the best fit is 0.97 in the 5.85–7 μm region. The weak inclination of the ellipses (i.e., their roundness at the scales of the plot) indicates that the two parameters are poorly correlated (Bevington & Robinson 1992). The linear correlation coefficient is equal to 0.034. In Figure 3(b), red iso-χ^2 contours are computed by fixing $T_{\rm rot}$ and OPR and then minimizing χ^2 with the coefficients of the polynomial and the water production rate left as free parameters. With respect to the iso-χ^2 contours computed with the previous method (superimposed in black), these χ^2 iso-contours extend a bit farther in $T_{\rm rot}$, while they coincide along the OPR dimension. This demonstrates that $T_{\rm rot}$ is weakly correlated with the coefficients of the polynomial, whereas OPR is not correlated. Quoted uncertainties in Table 1 and throughout the paper are 1σ (68% confidence level) uncertainties computed from the diagonal elements of the covariance matrix. They correspond approximately to the $\Delta\chi^2 = 1$ red contour in Figure 3(b). The joint confidence region for ($T_{\rm rot}$, OPR), delimited by the $\Delta\chi^2 = 2.3$ contour (Bevington & Robinson 1992), is not used here as these parameters are not physically linked.

Model fits with residuals are shown in Figures 4 and 5, for 71P/Clark and C/2004 B1 (LINEAR), respectively.

3.2. Water Modeling Results

In the case of 71P/Clark, model fitting was performed for two different extraction apertures along the slit, 3.″7 × 5.″6 (top of Figure 4) and 3.″7 × 17.″9 (bottom of Figure 4). For the small-extraction aperture, there is significant disagreement at 6.35–6.40 μm (this region was masked during the fitting procedure to obtain successful results in the other domains). The intensity of the water band is less intense than expected from modeling, resulting in negative residuals. This low intensity is puzzling. At low temperatures, the 6.40 μm peak arises mainly from the 1_{01}–1_{10} and 1_{11}–2_{02} lines, whereas the 6.50 μm peak comes mainly from the 1_{01}–2_{12} and 2_{12}–2_{21} lines. The ratio of their intensities I(6.40 μm)/I(6.50 μm) decreases with decreasing $T_{\rm rot}$ (see Figure 5 of Woodward et al. 2007), but reaches a constant value of $\sim$ 0.4–0.5 at low T and fluorescence equilibrium. For the large-extraction aperture, the discrepancy is shifted towards the 6.45–6.50 μm domain (Figure 4). Therefore, it is likely that the misfit in the 6.35–6.50 μm range is related to incorrect background subtraction and/or instrumental artifacts. Outside this spectral domain, the agreement between our model of H_2O emission and the *Spitzer* spectra of 71P/Clark is good.

The best fits to the spectra of 71P/Clark correspond to rotational temperatures $T_{\rm rot}$ of 5 ± 13 K (large-extraction aperture) and 14 ± 4 K (small-extraction aperture), both consistent with $T_{\rm rot}$< 18 K (similar values are found for OPR = 2.5 and 3.0). Indeed, the 6.50 μm peak is less intense than the 6.65 μm peak

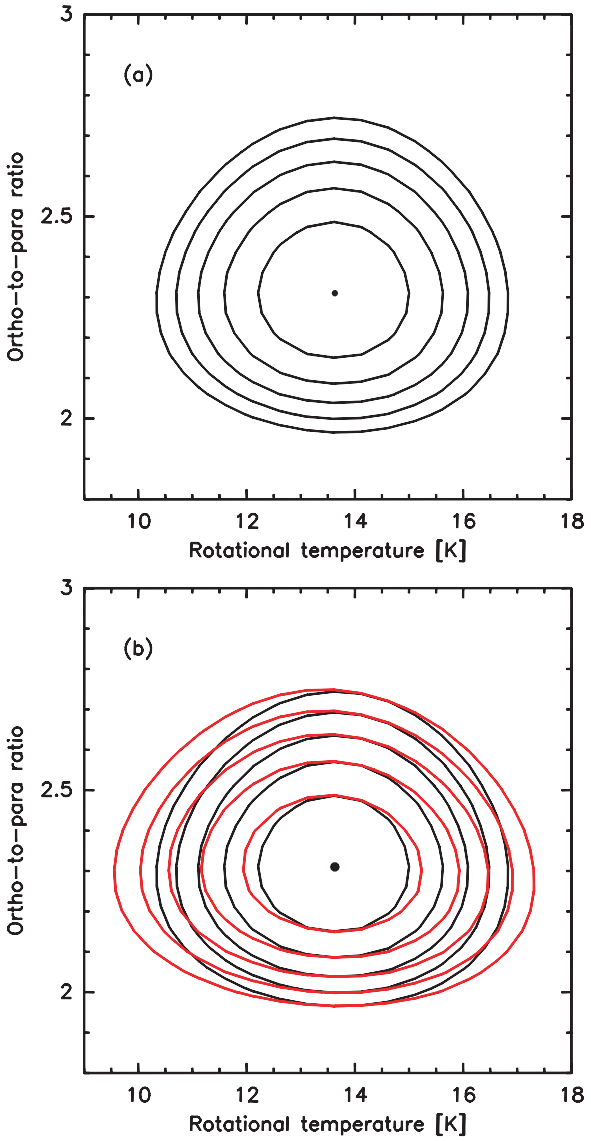

Figure 3. Contours showing the variation of χ^2 with $T_{\rm rot}$ and OPR in the region that provides the best fit to the C/2004 B1 (LINEAR) pre-perihelion spectrum. Iso-χ^2 contour levels correspond to increases in χ^2 by steps of 1 from the minimum value (denoted by small black dot). (*a*) The contours are calculated by holding the polynomial coefficients and the water production rate fixed at their optimum values. (*b*) The contours shown in red color are calculated by allowing those parameters to vary to minimize χ^2 for each pair of values of $T_{\rm rot}$ and OPR. Black contours are those shown in panel (*a*).

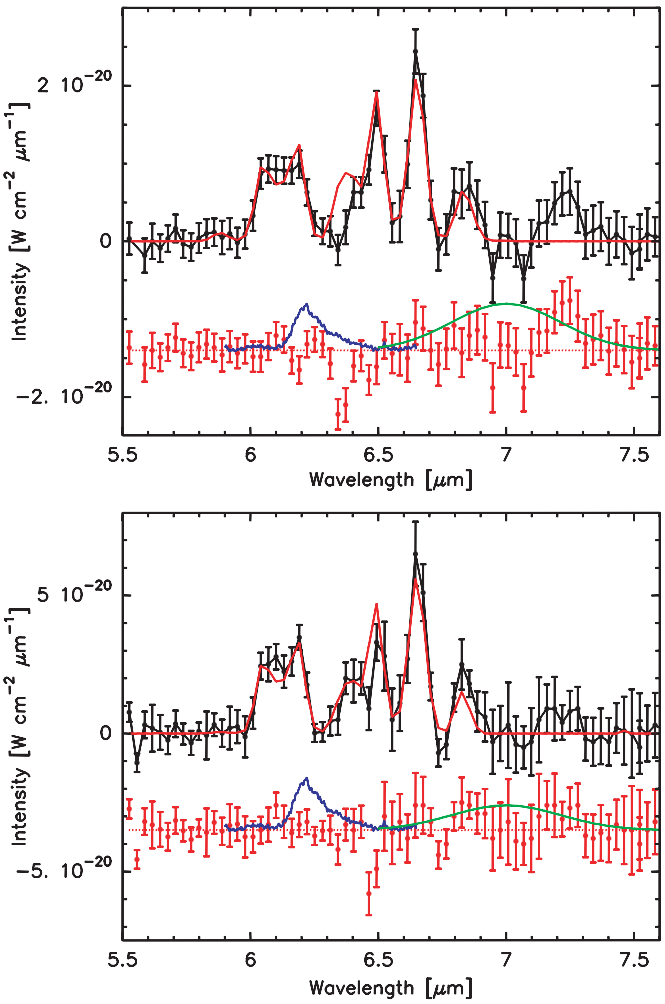

Figure 4. Model fit to the 2006 May 27.56 UT (pre-perihelion) spectra of comet 71P/Clark with extraction apertures of 3.″7 × 5.″6 (top) and 3.″7 × 17.″9 (bottom). Data are shown in black dots with error bars. The synthetic water spectrum obtained from model fitting with OPR = 3 is shown in red. The retrieved $T_{\rm rot}$ is 14 ± 4 K and 5 ± 13 K for the small and large apertures, respectively. The residual spectrum is shown in red on the bottom, on which are superimposed in arbitrary units an interstellar PAH spectrum typical of class A sources from Peeters et al. (2002; blue spectrum), and a model of carbonate emission from Lisse et al. (2006; green spectrum).

only for $T_{\rm rot} < 20$ K (see Figure 5 of Woodward et al. 2007, where the emergent intensity of the H_2O ν_2 band is plotted as a function of rotational temperature). The reverse was observed in *Spitzer* spectra of C/2003 K4 (LINEAR) from which $T_{\rm rot}$ values $\sim$ 30 K were determined (Woodward et al. 2007).

The signal-to-noise ratio achieved in the C/2004 B1 (LINEAR) pre-perihelion water spectrum ($\sim$50 in-band intensity on the 3.″7 × 17.″9 extraction aperture considered for model fitting) permits a determination of the water ortho-to-para ratio (OPR), as done from *Spitzer* spectra of C/2003 K4 (LINEAR; Woodward et al. 2007). The best fit, shown in Figure 5, corresponds to $T_{\rm rot} \simeq 14 \pm 2$ K and OPR = 2.31 ± 0.18. Also shown in Figure 5 is the best fit obtained with the OPR fixed at a value of 3. The χ^2 is increased by $\Delta\chi^2 = 10$ with respect to the best fit obtained with OPR = 2.31.

The agreement between our model and the *Spitzer* spectrum is excellent, except for the structure at 6.85 μm where the predicted intensity is lower than observed with a 2σ discrepancy. Taking the 6.05 μm peak as a reference since its intensity is weakly dependent upon $T_{\rm rot}$ and OPR (cf., Figures 5 and 6 of Woodward et al. 2007), the intensity ratio I(6.85 μm)/I(6.05 μm) slowly increases with increasing $T_{\rm rot}$ (and decreasing OPR) (Figures 5 and 6 of Woodward et al. 2007). The observed ratio would be typical of $T_{\rm rot} \sim$ 50 K. However, the relative intensities of the other peaks (in particular, I(6.65 μm)/I(6.05 μm) and I(6.18 μm)/I(6.05 μm)) are indicative of a low $T_{\rm rot}$. Model fitting to the 5.9–6.7 μm part of the spectrum yields the same results as those obtained from the whole spectrum. As discussed in Woodward et al. (2007), the band regions most sensitive to the OPR lie at 6.12 and 6.4 μm where the emission is dominated by para lines: model fitting with OPR = 3 results in excess emissions centered at 6.12 μm and 6.4 μm in the residuals. The discrepancy at 6.85 μm is likely related to instrumental effects or flaws in the background subtraction (the negative feature at 7 μm in the residuals is not explained either).

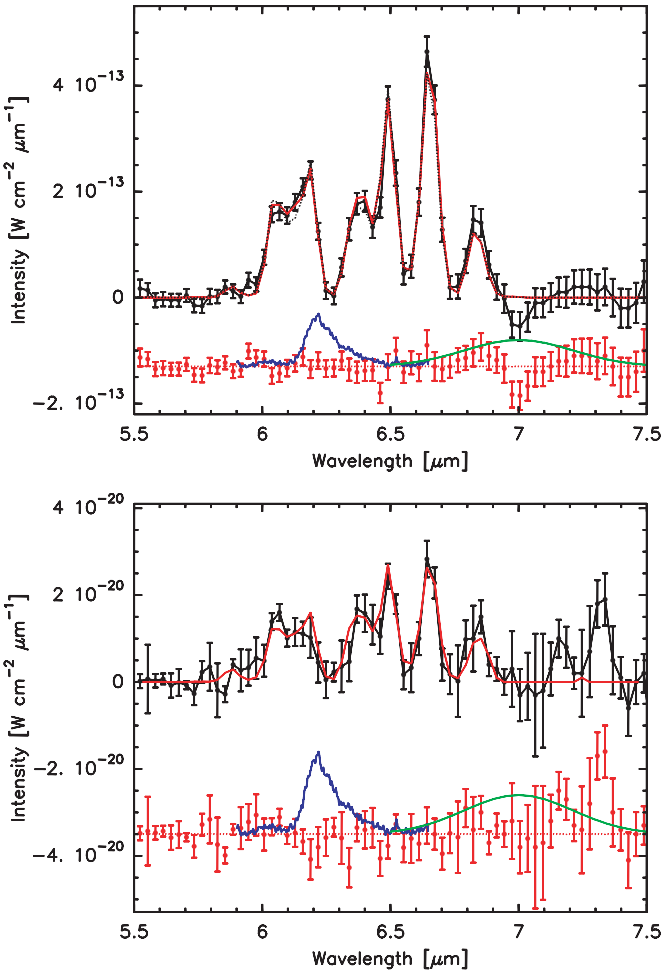

Figure 5. Model fits to the 2005 October 27.56 UT (pre-perihelion, top) and 2006 May 16.22 UT (post-perihelion, bottom) spectra of comet C/2004 B1 (LINEAR) obtained with an extraction aperture of 3.″7 × 17.″9. Data are shown in black dots with error bars, while other colored curves are as described in Figure 4. Model fitting to the pre-perihelion spectrum yields $T_{\rm rot} = 13.6 \pm 2.1$ K and OPR = 2.31±0.18. The best fit obtained with the OPR fixed to OPR = 3 ($T_{\rm rot} = 13.4$ K) is shown by a black dotted line. For the post-perihelion spectrum, the OPR is fixed to a value of 2.3, and the derived rotational temperature is $T_{\rm rot} = 23 \pm 4$ K.

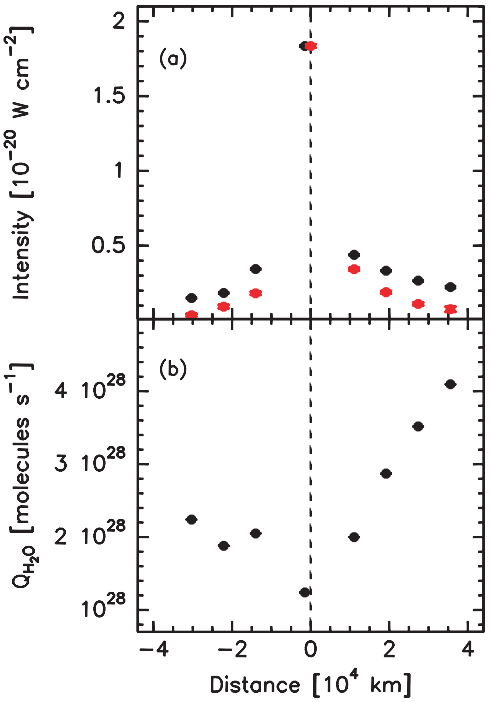

Figure 6. Distribution of water and dust as a function of offset, ρ, with respect to the nucleus position in C/2004 B1 (LINEAR) at $r_h = 2.2$ AU (pre-perihelion). Negative offsets correspond to southern extractions with respect to the peak in the surface brightness of the coma, Figure 1(a). (*a*) Total water ν_2 band intensity between 5.8 and 7 μm (black circles) and dust continuum (red circles) surface brightness determined from equivalent narrow-band continuum (divided by a factor of 17) measured at λ = 5.45 ± 0.08 μm. Extraction apertures are 5.″6 × 5.″6, except for the most central extraction which has an 5.″6 × 11.″1 aperture. For clarity, the central (offset = −1″) dust point has been shifted to an offset equal to zero. The water intensity varies as $\rho^{-1.13}$ for the southern extractions, and as $\rho^{-0.54}$ for the northern extractions, while the dust emission (average of the northern and southern coma values) decreases with increasing offset as $\rho^{-1.30}$. (*b*) The *Q*-curve, i.e., the apparent $Q(H_2O)$ production rates required to explain the H_2O band intensity at the different offsets in the assumption of a Haser parent molecule distribution.

The best-fit modeled spectrum for C/2004 B1 (LINEAR) post-perihelion is shown in Figure 5. For this model fitting, we fixed the ortho-to-para ratio to the value OPR = 2.3 derived from the pre-perihelion data. The derived rotational temperature is $T_{\rm rot} = 23 \pm 4$ K. A similar value ($T_{\rm rot} = 20$ K) is obtained with OPR = 3 (fit shown in Figure 2) and OPR = 2.5 ($T_{\rm rot} = 22$ K). The agreement between our model and the *Spitzer* spectrum is rather good. The residuals with respect to the observed spectrum do not show any excess emission in the wavelength range 5.8–7.1 μm of water ν_2 band emission.

3.3. Water Production Rates

From the intensity of the ν_2 H_2O band measured on the spectra, we computed the water production rates of 71P/Clark and C/2004 B1 (LINEAR) using a Haser model for the water density (Table 1). Because the observations of comet 71P/Clark were affected by pointing offsets due to uncertainties in the ephemeris (Section 2), the production rates retrieved from the intensities measured in a small (3.″7 × 5.″6) and large (3.″7 × 17.″9) extraction aperture were used as a complementary check to the pointing offsets. Consistent values for $Q(H_2O)$, equal to $(1.08 \pm 0.08) \times 10^{28}$ molecules s^{-1} and $(1.04 \pm 0.08) \times 10^{28}$ molecules s^{-1} for the small- and large-extraction apertures, respectively, are obtained applying offsets corresponding to the actual position of the nucleus with respect to the targeted position. This derived production rate for the 2006 perihelion is consistent with indirect estimations from the visual brightness at previous perihelia (Sekanina 1993).

The water production rate derived for C/2004 B1 (LINEAR) at $r_h = 2.21$ AU pre-perihelion is $Q(H_2O) = (1.03 \pm 0.02) \times 10^{28}$ molecules s^{-1}. At $r_h = 2.06$ AU post-perihelion, the measured $Q(H_2O)$ is $(4.74 \pm 0.42) \times 10^{27}$ molecules s^{-1}, which suggests that the comet was more active pre-perihelion. This later conclusion is consistent with measurements of the total visual magnitude m_v of the comet. For 2005 October 21 and 2006 May 17, i.e., at dates close to the *Spitzer* observations, values $m_v = 12.6$ and 12.4 are reported, which correspond to heliocentric visual magnitudes of 11.1 and 11.8, respectively (Green 2005, 2006).

Water production rates were computed assuming a Haser parent-molecule distribution for the water density with the parameters given in Section 3.1. The signal-to-noise ratio achieved for C/2004 B1 (LINEAR) pre-perihelion permits the investigation of the radial distribution of water throughout the IRS SL2 spectral map (Figure1(a)). The intensity of the ν_2 band along nine extractions is plotted as a function of offset

ρ in Figure 6(a). The ν_2 intensity varies as $\rho^{-0.54}$ north of the nucleus which suggests that the water distribution is extended in this direction. South of the nucleus, the intensity varies as $\rho^{-1.13}$, which is consistent with a Haser distribution. For comparison (Figure 6(a)), the surface brightness of the dust emission (derived from continuum measurements at 5.45 $\pm$ 0.08 μm in each of the nine apertures) decreases with increasing offset as $\rho^{-1.30}$ (southern and northern coma averaged).

The extended water distribution is best evidenced in the "*Q*-curve" (see Mumma et al. 2003) shown in Figure 6(b) which plots the water production required to explain the H_2O band intensity at the different offsets, assuming a Haser distribution. The apparent $Q(H_2O)$ increases by more than a factor of 2 from 1×10^4 km to 4×10^4 km. This extended distribution is suggestive of the presence of subliming icy grains in the coma of C/2004 B1 (LINEAR). At 2.1 AU from the Sun the lifetime of dirty ice grains ranges from 10^4–10^6 s for grains of radii 10^{-2}–1 cm (Beer et al. 2006). This lifetime range corresponds to displacements within the coma of typically 10^3–10^4 km prior to complete grain sublimation. The lifetime of pure ice grains is considerably larger (Beer et al. 2006). Our measurements are most easily explained if pure icy grains or ices mixed with poorly absorbing materials are present in the coma of comet C/2004 B1 (LINEAR). However, modeling of such sublimation processes is beyond the scope of this paper.

3.4. Rotational Temperatures

The measured rotational temperatures (Table 1) may not correspond to physical gas temperatures. As the water molecules expand in the coma, the rotational populations within the ground vibrational state relax to a cold fluorescence equilibrium. Thermal equilibrium breaks down at distances which depend on the density of the collisional partners (mainly H_2O molecules and electrons), and which are directly related to the water production rate. Given the low water production rate of 71P/Clark and C/2004 B1 (LINEAR), and the observational circumstances (field of view, slit offset), we may expect molecules with non-LTE rotational populations within *Spitzer* IRS SL2 slit. Using a model of water rotational excitation and the methodology explained in Woodward et al. (2007), we have computed synthetic ν_2 band profiles for the observing conditions of 71P/Clark and C/2004 B1 (LINEAR) from *Spitzer* and the field-of-view corresponding to the extraction apertures. Effective $T_{\rm rot}$ were derived by fitting the synthetic spectra with the same procedure as used for the observed spectra.

For 71P/Clark, the predicted effective $T_{\rm rot}$ at 8″from the nucleus is 11–12 K for a kinetic temperature $T_{\rm kin}$ in the range 10–50 K and $x_{ne} = 1$, where x_{ne} is a multiplying factor to the electron density normalized to the Giotto 1P/Halley measurements. If our observations had been executed with the slit centered on the nucleus, we would have expected $T_{\rm rot} = 25$ to 29 K with these model parameters. These results are for an aperture of 3.″7 $\times$ 17.″9, but similar numbers are obtained for a 3.″7 $\times$ 5.″6 aperture: 31–39 K on nucleus, 12–13 K for an offset of 8″. The size of the collisional region where water molecules are thermalized to the gas kinetic temperature is small with respect to the field of view, hence the predicted rotational temperature is weakly sensitive to the assumed $T_{\rm kin}$. A relatively high $T_{\rm rot}$ is expected for a slit centered on the nucleus because molecules excited by collisions with hot electrons have a significant contribution to the signal. Rotational temperatures measured in 71P/Clark (14 $\pm$ 4 K and 5 $\pm$ 13 K for the small and large apertures, respectively) are consistent with modeling.

Model calculations pertaining to the observational circumstances of the C/2004 B1 (LINEAR) pre-perihelion data predict $T_{\rm rot}$ = 17–19 K for a 3.″7 $\times$ 17.″9 aperture and kinetic temperatures of 10–50 K. Note that low gas temperatures may be expected for this weakly active (Section 3.3) comet observed at 2.1–2.2 AU from the Sun. Overall, the agreement with the measured $T_{\rm rot}$ value (13.6 $\pm$ 2.1 K) is satisfactory.

In the case of C/2004 B1 (LINEAR) post-perihelion, the expected $T_{\rm rot}$ for a 3.″7 $\times$ 17.″9 extraction centered on the nucleus is $T_{\rm rot} = 17$ K assuming $T_{\rm kin} = 30$ K, with little dependency on the assumed $T_{\rm kin}$ since water molecules with non-LTE rotational populations are sampled. The measured $T_{\rm rot}$ of 23 $\pm$ 4 K is consistent with the model within 2σ. A better agreement could be obtained by increasing the electron density through the $x_{ne} = 1$ parameter.

3.5. Ortho-to-para Ratio in C/2004 B1 (LINEAR)

The ortho-to-para ratio of 2.31 $\pm$ 0.18 measured in C/2004 B1 (LINEAR) corresponds to a spin temperature $T_{\rm spin} = 26^{+3}_{-2}$ K. The ortho-to-para ratio in water has been measured in a dozen of comets (see Bonev et al. 2007, for a compilation of measurements before 2007), and ranges from $\sim$ 1.8 to the equilibrated value of 3 ($T_{\rm spin}$ from $\sim$ 23 to $>$ 40 K). The OPR measured in C/2004 B1 (LINEAR) is in the low range of measured values in Oort cloud comets, yet comparable to OPR values reported by Mumma et al. (1988) and Dello Russo et al. (2005) for comets 1P/Halley and C/2001 A2 (LINEAR). Our new measurement for C/2004 B1 (LINEAR) suggests that OPR variation clearly exists among the population of Oort cloud comets.

The meaning of nuclear spin temperatures in cometary molecules is puzzling (Kawakita et al. 2004; Crovisier 2007). Nuclear spin temperatures may be related to the thermal conditions experienced by the molecules since their incorporation into cometary nuclei, or connected to their formation conditions and subsequent OPR re-equilibration in the solar nebula. Kawakita et al. (2004) have shown that there is no clear trend between the nuclear spin temperatures, production rate, heliocentric distance and orbital period of the comet, suggesting that the nuclear spin temperature is pristine (Kawakita et al. 2004). The measurement of the OPR (and corresponding nuclear spin temperature) in C/2004 B1 (LINEAR) is derived from observations conducted when the comet was at a heliocentric distance, $r_h = 2.21$ AU. This heliocentric distance is intermediate between the range r_h = 0.8–1.2 AU, where most OPR measurements were acquired, and the measurement in C/1995 O1 (Hale-Bopp) at 2.9 AU from the Sun. Our *Spitzer* measurement provides a new data point for future investigations of $T_{\rm spin}$ variations with heliocentric distance based on a statistically significant data set.

3.6. Residual Emissions

The modeled water spectrum wholly accounts for the emission in excess of the dust continuum background in the two comets (Figures 4 and 5). There is no emission excess at 6.2 μm that could be attributed to PAH emission. There is not significant evidence for moderately broad ($\Delta\lambda \simeq 0.5$ μm) emission peaking at 7.0 μm (arising from asymmetric stretching vibration of C–O) that could be due to carbonates minerals (Kemper et al. 2002; Crovisier & Bockelée-Morvan 2008). Such emission, if present, would have made the 6.85 μm peak of the H_2O band of less contrast than observed. In addition if carbonates where present, other narrow ($\Delta\lambda \lesssim 0.2$ μm) emission features near

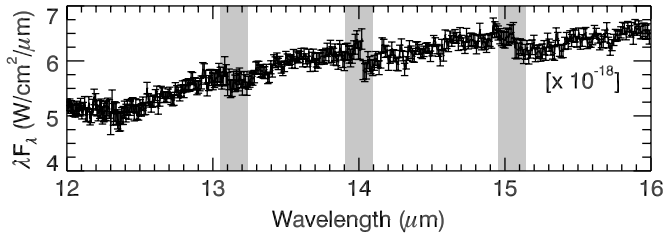

Figure 7. *Spitzer* IRS short-high (SH) spectra of comet C/2004 B1 (LINEAR) over the wavelength range from 12.0 μm to 16.0 μm where narrow resonances from the out-of-plane and in-plane bending mode of the $(CO_3)^{2-}$ ion in carbonate species are expected (Kemper et al. 2002). The gray vertically shaded areas indicate the wavelength locations of the spectral-order overlap in the instrument and the discontinuity of the spectra in these regions are artifacts. The IRS spectra are featureless in the wavelength regions of the carbonate resonances (narrow features near 12.7 μm and 14.8 μm), suggesting that carbonates are not present with large abundance, if at all, in the emitting coma materials.

12.7 μm and 14.8 μm should be present (Kemper et al. 2002). The IRS spectra of comets C/2004 B1 (LINEAR) and 71P/Clark over this wavelength interval are featureless, Figure 7. Thus, carbonates are not present (or significantly abundant) in the comet comae created through quiescent sublimation processes or dermal jets from isolated active areas on the nucleus based on analysis of *Spitzer* spectra of three comets.

Excess emission is present at 7.1–7.3 μm in the spectrum of 71P/Clark, and between 7.15 and 7.45 μm, peaking at 7.32 μm in the post-perihelion spectrum of C/2004 B1 (LINEAR) (Figures 4 and 5). Excess emission near 7.3 μm was also observed in the *Spitzer* spectrum of C/2003 K4 (LINEAR) (Woodward et al. 2007). The emission feature observed in C/2004 B1 (LINEAR) post-perihelion closely resembles that observed for C/2003 K4 (LINEAR), but is much more intense relative to the intensity of the water band than in C/2003 K4 (LINEAR): $\sim$ 10% the intensity of the water band in the post-perihelion spectrum of C/2004 B1 (LINEAR), $\sim$ 2% in C/2003 K4 (LINEAR; Woodward et al. 2007). Its contrast with respect to the continuum background is also more important in C/2004 B1 (LINEAR). The feature is not present in the pre-perihelion spectrum of C/2004 B1 (LINEAR). This suggests that the feature is not related to the absolute brightness of the comet. As discussed in Woodward et al. (2007), the origin of this feature is unclear. Based on examination of spectral extractions of standard stars used to calibrate the IRS campaign, this feature is not likely an instrumental artifact, although we cannot completely exclude this possibility.

4. CONCLUSION

We have presented *Spitzer* IRS spectra of the water ν_2 fundamental vibrational band near 6.5 μm in the Jupiter-family comet 71P/Clark and the dynamically new comet C/2004 B1 (LINEAR). Modeling of the IR spectra using a fluorescence model of the water emission yielded rotational temperature and production rate measurements. The measured low rotational temperatures are consistent with water excitation models which predict that water molecules within the *Spitzer* IRS slit have partially relaxed (non-LTE) rotational populations. The water ortho-to-para ratio (OPR) was constrained to 2.31 ± 0.18 in C/2004 B1 (LINEAR) from its pre-perihelion spectrum observed with a high signal-to-noise ratio. The corresponding spin temperature $T_{\rm spin} = 26^{+3}_{-2}$ K is in the low range of measured values in other Oort cloud comets. In addition, the spatial distribution of water observed (pre-perihelion) in the northern coma of C/2004 B1 (LINEAR) is more extended than that expected for nucleus outgassing which suggests the presence of subliming icy grains.

Although the 5.8–7.6 μm spectral domain is rich in spectral signatures of gaseous compounds and minerals our spectra show no incontrovertible evidence for carbonates, or PAH emission. Thus, reported claims that these astrobiologically significant species are present (e.g., Lisse et al. 2007, 2006) remain controversial (i.e., Crovisier & Bockelée-Morvan 2008; Bockelée-Morvan et al. 2007; Woodward et al. 2007). As seen in comet C/2003 K4 (LINEAR) (Woodward et al. 2007), residual emission at 7.1–7.3 μm is present in spectra of 71P/Clark and C/2004 B1 (LINEAR) whose origin is unclear.

This work is based on observations made with the *Spitzer Space Telescope*, which is operated by the Jet Propulsion Laboratory, California Institute of Technology under a contract with NASA. Support for this work was provided by NASA through an award issued by JPL/Caltech. Support for this work was also provided by NASA through contracts 1263741, 1256406, and 1215746 issued by JPL/Caltech to the University of Minnesota. C.E.W. also acknowledges support from the National Science Foundation grant AST-0706980. We thank the anonymous referee for helpful comments, and N. Biver, D. E. Harker and D. Pelat for enlightening discussions.

Facilities: Spitzer (IRS)

REFERENCES

A'Hearn, M. F., et al. 2005, Science, 310, 258
A'Hearn, M. F., Schleicher, D. G., Feldman, P. D., Millis, R. L., & Thompson, D. T. 1984, AJ, 89, 579
Beer, E. H., Podolak, M., & Prialnik, D. 2006, Icarus, 180, 473
Bevington, P. R., & Robinson, D. K. 1992, Data Reduction and Error Analysis for the Physical Sciences (2nd ed,; New York: McGraw-Hill), 212
Biver, N., et al. 2007, Planet. Space Sci., 55, 1058
Bockelée-Morvan, D., & Crovisier, J. 1989, A&A, 216, 278
Bockelée-Morvan, D., Woodward, C. E., & Kelley, M. S. 2007, BAAS, 38, 508
Bockelée-Morvan, D., Crovisier, J., Mumma, M. J., & Weaver, H. A. 2004, in Comets II, ed. M. Festou, H. U. Keller, & H. A. Weaver (Tucson: Univ. of Arizona Press), 391
Bonev, B. P., Mumma, M. J., Villanueva, G. L., Disanti, M. A., Ellis, R. S., Magee-Sauer, K., & Dello Russo, N. 2007, ApJ, 661, L97
Bonev, T., et al. 2007, arXiv:0704.3834
Crovisier, J., & Bockelée-Morvan, D. 2008, Icarus, 195, 938
Crovisier, J., et al. 1997, Science, 275, 1904
Dello Russo, N., Bonev, B. P., DiSanti, M. A., Mumma, M. J., Gibb, E. L., Magee-Sauer, K., Barber, R. J., & Tennyson, J. 2005, ApJ, 621, 537
Crovisier, J. 2007, arXiv:astro-ph/0703785
Disanti, M. A., & Mumma, M. J. 2008, Space Sci. Rev.
Gehrz, R. D., et al. 2007, Rev. Sci. Instrum., 78, 011302
Green, D. 2005, Int. Comet Q., 136, 271
Green, D. 2006, Int. Comet Q., 139, 121
Gulkis, S., et al. 2007, Space Sci. Rev., 128, 561
Houck, J. R., et al. 2004, ApJS, 154, 18
Kawakita, H., Watanabe, J.-i., Furusho, R., Fuse, T., Capria, M. T., De Sanctis, M. C., & Cremonese, G. 2004, ApJ, 601, 1152
Kelley, M. S., et al. 2006, ApJ, 651, 1256
Kemper, F., Jager, C., Waters, L. B. F. M, Hennning, Th., Molster, F. J., Barlow, M. J., Lim, T., & de Koter, A. 2002, Nature, 415, 295
Lamy, P. L., Toth, I., Fernandez, Y. R., & Weaver, H. A. 2004, in Comets II, ed. M. Festou, H. U. Keller, & H. A. Weaver (Tucson: Univ. of Arizona Press), 223
Lisse, C. M., Kraemer, K. E., Nuth, J. A., Li, A., & Joswiak, D. 2007, Icarus, 187, 69
Lisse, C. M., et al. 2006, Science, 313, 635
Marsden, B. G. 2004, MPEC, 2004-B73
Meech, K. J., Hainut, O. R., & Marsden, B. G. 2004, Icarus, 170, 463

Mumma, M. J., Blass, W. E., Weaver, H. A., & Larson, H. P. 1988, in The Formation and Evolution of Planetary Systems, ed. H. A. Weaver, F. Paresce & L. Danly (Baltimore, MD: STScI), 157
Mumma, M. J., DiSanti, M. A., dello Russo, N., Magee-Sauer, K., Gibb, E., & Novak, R. 2003, Adv. Space Res., 31, 2563
Nakano, S. 2006a, Yamamoto Circ., 2500
Nakano, S. 2006b, NK 1618 (Sumoto: Center for Astrodynamics, Oriental Astronomical Association), http://www.oaa.gr.jp/oaacs/nk/nk1618.htm
Peeters, E., Hony, S., Van Kerckhoven, C., Tielens, A. G. G. M., Allamandola, L. J., Hudgins, D. M., & Bauschlicher, C. W. 2002, A&A, 390, 1089
Sandford, S. A., et al. 2006, Science, 314, 1720
Sandford, S. A., & Brownlee, D. E. 2007, Science, 317, 1680
Sekanina, Z. 1993, A&A, 277, 265
Spencer, M. K., & Zare, R. N. 2007, Science, 317, 1680c
Szutowicz, S. 1999, in IAU Colloq. 173, Evolution and Source Regions of Asteroids and Comets, ed. J. Svoren, E. M. Pittich, & H. Rickman (Tatranska Lomnica, Slovak Republic: Astron. Inst. Slovak Acad. Sci.), 259
Werner, M. W., et al. 2004, ApJS, 154, 1
Wirick, S., et al. 2007, Lunar Planet. Inst. Conf. Abstr., 38, 1534
Woodward, C. E., et al. 2008, Lunar Planet. Inst. Contribution, 1045, 8013
Woodward, C. E., Kelley, M. S., Bockelée-Morvan, D., & Gehrz, R. D. 2007, ApJ, 671, 1065
Young, J. 2004, IAU Circ., 8279